

## Thermally induced interface degradation in (111) Si/SiO<sub>2</sub> traced by electron spin resonance

A. Stesmans and V. V. Afanas'ev

Department of Physics, University of Leuven, 3001 Leuven, Belgium

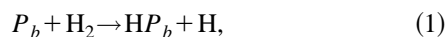
(Received 3 June 1996)

Thermal post-oxidation interface degradation in (111) Si/SiO<sub>2</sub> has been isolated by electron-spin resonance (ESR) as a permanent  $P_b$  (Si≡Si<sub>3</sub>) interface defect creation. This process, initiating from ~640 °C onward, reveals interface breakdown on an atomic scale as interfacial SiO bond rupture. The crucial creation step has been isolated as thermal cycling in an O-free ambient. Once created, the new  $P_b$  system exhibits similar fully reversible H passivation-depassivation kinetics as the preexisting one, naturally introduced during oxidation. ESR is herewith raised to a powerful probe for Si/SiO<sub>2</sub> degradation. [S0163-1829(96)51340-8]

As crucial transistor SiO<sub>2</sub> gate oxides enter the sub 5-nm region, there is more concern than ever about the quality of the nonscaling (111) Si/SiO<sub>2</sub> interface. The incorporation of electrically active interface defects, induced by lattice mismatch<sup>1</sup> during oxidation, is a long known Achilles' heel<sup>2</sup> of the superb Si/SiO<sub>2</sub> structure. Atomic identification of these coordination defects—in particular those responsible for current degradation—has received much attention.<sup>3</sup>

The key information<sup>3-7</sup> comes from electron spin resonance (ESR), which has been applied successfully to at least part of these defects. In standard (111) Si/SiO<sub>2</sub>, only one type of ESR-active defect is encountered,<sup>4</sup> called  $P_b$ . It has been identified as an unpaired electron in a dangling  $sp_{[111]}$ -like hybrid on an interfacial Si atom trivalently backbonded to Si atoms in the bulk, pointing into a microvoid. More specifically only the [111]  $P_b$  species with the unpaired hybrid  $\perp$  (111) Si/SiO<sub>2</sub> interface occurs normally.<sup>3,4</sup> From a symbiotic combination of ESR with electrical measurements, a close correlation was concluded<sup>3</sup> between the  $P_b$  density [ $P_b$ ] and the interface trap density  $D_{it}$ . From early on, in the Si era, the interface defects were technologically mastered—either deliberately or inadvertently—through inactivation by hydrogen, which is admitted to simply lead to the formation of  $HP_b$  entities.<sup>1,8</sup> The interaction with H thus emerged as a major thermochemical issue.

Intensive ESR analysis<sup>9-11</sup> of the H- $P_b$  interaction kinetics inferred a transparent fully reversible H- $P_b$  interaction scheme. Passivation and depassivation (studied in the 230–260 °C and 500–590 °C ranges, respectively) are described by the reactions



proceeding with activation energy  $E_a \approx 1.66$  and 2.56 eV, respectively. The net result of both steps is simply the thermal dissociation of the H<sub>2</sub> molecule.<sup>11</sup> Supported by theoretical insight,<sup>12</sup> this lucid picture soon became accepted as definitive. Basic ingredients of the simple picture are full reversibility and  $P_b$  entity stability: the  $P_b$  sites are formed during thermal oxidation and the total density of defect entities [ $P_b$ ] +  $HP_b$ —passivated by H or not—remains fixed. The latter was thought evident from some singular depassivation experiments at elevated temperatures<sup>10</sup> (675–850 °C)

based on ESR signal height monitoring; this method fails, however, in the case of  $P_b$ , it turns out.<sup>13</sup> So, only one  $P_b$  generation mechanism,  $HP_b$  dissociation, was concluded.

However, recent extended ESR work<sup>13</sup> on  $P_b$  passivation places the simple scheme in a less ideal perspective. This prompted reanalysis of the complementary  $HP_b$  dissociation kinetics, during which it emerged that the reversible H- $P_b$  interaction mechanism is only half of the story. Just in the  $T$  range where depassivation is readily completed, an irreversible mechanism is found to initiate substantial  $P_b$  creation *vis-à-vis* activation occurring in the first mechanism. This is reported here. It concerns a clear structural isolation of postoxidation anneal (POA) induced interface degradation—an effect of clear relevance to device technology that has previously been encountered electrically in varying circumstances.<sup>14</sup> Once created, the newly formed  $P_b$  sites are stable, their H-interaction kinetics from then on fully complying with the simple H- $P_b$  passivation/dissociation scheme inferred from their counterparts naturally incorporated during oxidation.

Si slices of 2×9 mm<sup>2</sup> each were cut from commercial 2-in.-diam two-side polished float zone (111) Si wafers (>100 Ω cm,  $p$  type). After appropriate cleaning, these were thermally oxidized in a laboratory setup at ~970 °C (1.1 atm O<sub>2</sub>; 99.999%; oxide thickness  $d_{ox} \sim 42$  nm) terminated by cooling to room temperature (~20 min) in the same ambient (more details are given elsewhere<sup>2</sup>). This was followed by a ~40-min treatment in H<sub>2</sub> (1.1 atm; 99.9999%) at 405 °C in order to passivate all<sup>10,13</sup>  $P_b$  [cf. Eq. (1)], as affirmed by ESR. Finally, samples were submitted to a 62-min annealing in diffusion-pumped vacuum ( $\leq 4 \times 10^{-7}$  Torr) at desired temperatures in the range 480 °C–1135 °C. The accuracy reached on  $T$  is  $\leq 0.3\%$ , with a uniformity over the sample space better than 0.5 °C.

Conventional absorption mode ESR (~20.6 GHz) measurements were carried out at 4.3 K. Modulation field amplitude (0.25 G; 100 kHz) and microwave power levels were reduced to such levels for which the signal response was linear. All spectra were taken with the applied magnetic field  $\mathbf{B} \perp$  (111) Si/SiO<sub>2</sub> interface (within 3°), corresponding to the smallest linewidth position as the  $g$  spread effect is then minimized. This assures optimum sensitivity and spectral comparison. Unlike previous work,<sup>9,10</sup> spin densities were determined by double numerical integration of the

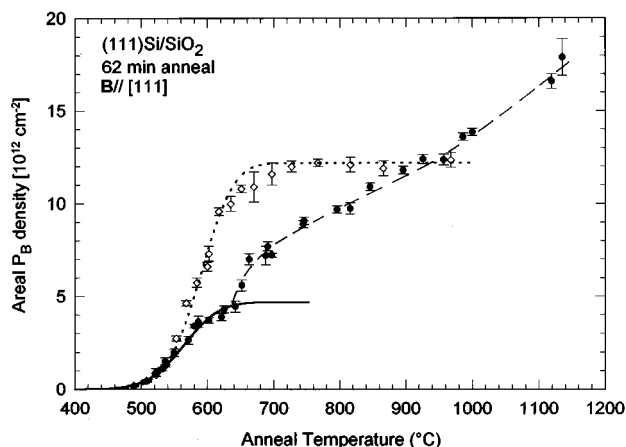


FIG. 1. Isochronal generation of ESR-active  $P_b$  defects in standard (111) Si/SiO<sub>2</sub>. (●): Each datapoint is obtained on a freshly oxidized ( $\sim 970^\circ\text{C}$ ) Si/SiO<sub>2</sub> structure, subsequently passivated in H<sub>2</sub> (1.1 atm H<sub>2</sub>; 405 °C;  $\sim 40$  min). (◇): Obtained on one sample, initially vacuum annealed at 967 °C for  $\sim 1$  h, where each isochronal annealing step is preceded by exhaustive passivation in H<sub>2</sub> (405 °C). All data points shown represent averages over four to six measurements. The error bars shown indicate the spread. Solid and dotted curves represent fits of Eq. (3). The dashed line is a guide to the eye.

absorption-derivative spectra relative to one fixed isotropic Si:P spin standard signal ( $g = 1.99869 \pm 0.00002$ ) recorded in one trace. Absolute and relative accuracy on measured spin densities is estimated at  $\sim 10\%$  and  $5\%$ , respectively. The increasing ESR linewidth and line-shape alterations with increasing  $P_b$  due to the strengthening dipolar interaction<sup>15</sup> requires care about the  $B$  integration range; This has been fixed at  $\sim 54$  G, centered at the  $P_b$  signal, appropriate for the highest  $[P_b]$ . Typically, about ten Si slices were stacked in an ESR sample.

The key results are assembled in Fig. 1, showing the isochronal (62 min)  $P_b$  generation by vacuum annealing in standard thermal (111) Si/SiO<sub>2</sub>. Of prime interest are the solid symbol data, each point pertaining to a freshly oxidized ( $\sim 970^\circ\text{C}$ ;  $d_{\text{ox}} \approx 42$  nm) and subsequently fully H passivated (1.1 atm H<sub>2</sub>; 405 °C;  $\sim 40$  min) sample (henceforth referred to as the fresh-oxide set). According to previous  $P_b$  ESR reactivation analysis (in the range 500 °C–595 °C), this should be solely a matter of dissociation of HP<sub>b</sub> entities, expected to be described by the first-order kinetics relation<sup>10</sup>

$$P_b/N_0 = 1 - \exp(-k_d t). \quad (3)$$

Here,  $N_0$  is the initial concentration of HP<sub>b</sub> centers (maximum number of recoverable ESR-active  $P_b$ s),  $t$  is the anneal time, and  $k_d = k_{\text{do}} \exp(-E_d/kT)$  is the rate constant ( $k$  is Planck's constant);  $E_d$  represents the activation energy for dissociation and  $k_{\text{do}}$  and pre-exponential factor, previously determined as  $E_d = 2.56 \pm 0.06$  eV and  $k_{\text{do}} \sim 1.2 \times 10^{12} \text{ s}^{-1}$ . The (ESR-active)  $P_b$  density would thus recover exponentially with increasing  $T$ , leveling off at  $N_0$  for  $T \geq 600^\circ\text{C}$ —in contrast with present observations showing little trend of a plateau. Instead, the data, spanning the range 480 °C–1135 °C, exhibit three characteristic features: (1) an

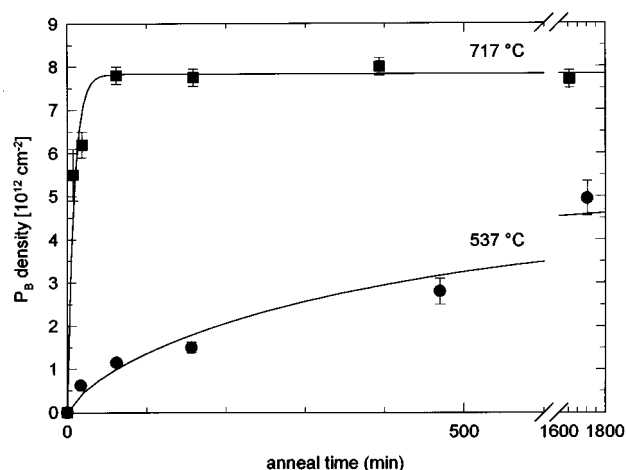


FIG. 2. Isothermal production of (ESR-active)  $P_b$  defects in standard (111) Si/SiO<sub>2</sub> (1.1 atm O<sub>2</sub>;  $\sim 967^\circ\text{C}$ ;  $d_{\text{ox}} \approx 42$  nm). For each  $T$ , data are obtained through cumulative stepwise annealing in vacuum of one sample initially exhaustively passivated in H<sub>2</sub> (1.1 atm H<sub>2</sub>; 405 °C;  $\sim 40$  min). The curves are guides to the eye.

exponential-like increase in the range 480 °C–600 °C; (2) a general monotonical increase in  $[P_b]$ , interrupted, however, by a weak though significant kink in the range 600 °C–650 °C; (3) a prominent monotonical increase in  $[P_b]$  above 650 °C, with no indication for saturation up to 1135 °C. It then remains to trace the underlying physics.

The interpretation of the lower  $T$  range ( $\leq 640^\circ\text{C}$ ) may still appear straightforward. Very informative here is the kink feature, which, when looked at from the low  $T$  side, is indicative of the onset of a leveling off at a  $P_b$  density of  $4.5\text{--}5 \times 10^{12} \text{ cm}^{-2}$ . This together with the initial exponential-like rise in  $[P_b]$ , leaves little doubt that the  $T \leq 640^\circ\text{C}$  data concern the known simple HP<sub>b</sub> dissociation mechanism, i.e., activation of preexisting HP<sub>b</sub> entities. Indeed, the  $T \leq 640^\circ\text{C}$  data may readily be fitted by Eq. (3) when complemented<sup>13</sup> by the existence of a spread  $\sigma_{E_d}$  in  $E_d$ . The fitted solid curve corresponds to the values  $E_d = 2.63 \pm 0.04$  eV,  $\sigma_{E_d} = 0.105 \pm 0.01$  eV, and  $N_0 = (4.7 \pm 0.2) \times 10^{12} \text{ cm}^{-2}$ , where the previous value<sup>10</sup>  $k_{\text{do}} = 1.2 \times 10^{12} \text{ s}^{-1}$  has been adopted.

In fitting, the initial  $N_0$  density might be left as a fitting parameter. Instead,  $N_0$  was determined experimentally through exhaustive dehydrogenation for  $\sim 29$  h at 537 °C—a value in the  $T$  range devoid of any noticeable admixing of the high- $T$   $P_b$  generation process—resulting in  $N_0 = (4.9 \pm 0.4) \times 10^{12} \text{ cm}^{-2}$  (see Fig. 2). That value is in reassuring agreement with the value  $[P_b] = 4\text{--}5 \times 10^{12} \text{ cm}^{-2}$  measured<sup>2</sup> on as-oxidized (111) Si/SiO<sub>2</sub> all over the oxidation range  $T_{\text{ox}} = 100^\circ\text{C}$ –1000 °C, suggesting that in the as-oxidized state, most  $P_b$  entities are not left passivated by H. It advances this value as the true number of  $P_b$  defects naturally incorporated in thermal (111) Si/SiO<sub>2</sub> during oxidation. The data then strikingly reveal that from  $\sim 640^\circ\text{C}$  onward, a second  $P_b$  generation mechanism enters,  $[P_b]$  monotonically increasing with no trend for leveling out; at  $\sim 950^\circ\text{C}$ , about  $7.6 \times 10^{12} \text{ cm}^{-2}$   $P_b$  have additionally been generated, while at 1135 °C,  $[P_b]$  has almost quadrupled.

This second process is identified as a  $P_b$  creation process

*vis-à-vis* activation ( $HP_b$  dissociation, the first generation mechanism). The evidence comes from a second set of 62-min vacuum anneal data (open symbols) shown in Fig. 1. This set was obtained on one state of the art oxidized sample submitted at once to a high- $T$  vacuum anneal at 968 °C for  $\sim 1$  h, exhibiting, as expected (cf. first data set), a  $P_b$  density of  $(12.3 \pm 0.4) \times 10^{12} \text{ cm}^{-2}$ . Each vacuum anneal step measurement is preceded by exhaustive passivation in  $\text{H}_2$ . The remarkable finding here is that this generation sequence, though on an enlarged scale, mirrors the simple  $HP_b$  dissociation mechanism exposed by the previous fresh-oxide data below  $\sim 640$  °C. The level of exhaustive  $HP_b$  dissociation—the initial value  $\sim 12.3 \times 10^{12} \text{ cm}^{-2}$ —is now clearly exposed by the extended plateau. Accordingly, the data may be well fitted by Eq. (3), as shown by the dotted curve. This indicates that  $P_b$  has initially (at 968 °C) been created, and is permanent in that the density of new  $P_b$  entities either passivated by H or not remains unaffected by subsequent treatment in an O-free ambient at any lower  $T$ . The extent of the process may be quantified (in terms of  $[P_b]$ ) in Fig. 1 by the dashed line, relative to the natural  $N_0 = 4\text{--}5 \times 10^{12} \text{ cm}^{-2}$  “baseline.”

Significantly, the very same effects have been observed when, instead of in vacuum, POA is carried out in inert ambient, i.e.,  $N_2$ . In sharp contrast, no  $P_b$  creation is observed in an oxygen-rich ambient. This complies with the observation that the created  $P_b$  are affected by reoxidation which is the way to eliminate them. This is not surprising, perhaps, as it just reestablishes an (inwardly moved) pristine Si/SiO<sub>2</sub> interface, characterized by the natural  $P_b$  density  $N_0$ . Two main conclusions follow. First, the second  $P_b$  generation process is uncovered as a truly irreversible  $P_b$  creation, where annealing in an O-deficient ambient at  $T \geq 660$  °C constitutes the crucial step—the very same conclusion as reached for oxide degradation.<sup>16</sup> Such annealing creates new  $P_b$  (e.g.,  $N_C \approx 7.6 \times 10^{12} \text{ cm}^{-2}$  at 960 °C), in densities  $N_C$  gradually increasing with  $T$ ; these appear in addition to the preexisting  $P_b$  system of  $N_0 = 4\text{--}5 \times 10^{12} \text{ cm}^{-2}$  naturally incorporated during oxidation. Second, after creation, the added  $P_b$  baths of density  $N_C + N_0$  behave as one uniform  $P_b$  system in a fully reversible way with respect to the H-interaction mechanism [cf. Eqs. (1) and (2)].

The creation mechanism proceeds rapidly, as illustrated in Fig. 2. Isothermal vacuum annealing at 717 °C reveals that  $P_b$  generation jumps to “saturation,” that is, creation of  $N_C \approx 3.0 \times 10^{12} P_b \text{ cm}^{-2}$  in addition to the depassivation of the  $N_0 \sim 4.8 \times 10^{12} \text{ cm}^{-2}$  preexisting  $HP_b$  entities, within about  $\frac{1}{2}$  h to remain constant for higher anneal times up to 28 h. The process proceeds faster with increasing  $T$ .

It may be useful to add that while the results presented so far were obtained using a laboratory-type thermal setup, some experiments have been repeated on samples fully cycled in an industrial facility,<sup>17</sup> with identical results. It underscores the universal character of the reported phenomena, i.e., not pertaining to some type of exotic oxides produced and handled in a nonrepresentative thermal facility.

The mechanism unveiled here is clearly (the) one of thermally induced interface degradation, a specific component of oxide-interfacial degradation of Si/SiO<sub>2</sub> structures and long recognized electrically.<sup>1,16</sup> It is likely that interface and oxide degradation have a common physical origin. In fact, the

present results are seen as providing the closing link for consistent picturing of Si/SiO<sub>2</sub> degradation.

Such a model should be based on and rigorously account for all essential facts regarding thermal Si/SiO<sub>2</sub> growth and degradation. In short, these include the following. (1)  $P_b$  defects are mismatch-induced centers, strongly correlated with interface stress.<sup>2</sup> (2) Standard oxidation of Si (800 °C–900 °C; 1 atm O<sub>2</sub>) is a terrace-attacking process, with little flow of interface steps,<sup>18</sup> that is, it occurs by oxidizing discrete monolayers (not preferentially steps); the initial step morphology is thus not improved. (3) In contrast, the etching of Si at the Si/SiO<sub>2</sub> interface through volatile SiO extraction occurs preferentially at steps;<sup>18</sup> it would tend to reduce the step density. (4) The average step spacing at the (111) Si/SiO<sub>2</sub> interface is drastically reduced (order of magnitude) by high- $T$  annealing in inert ambient (1050 °C; N<sub>2</sub>; 1 h),<sup>19</sup> the effect decreasing<sup>20</sup> with  $T$  [nonoxidizing conditions are flattening, in compliance with (3)]. (5) As electrically detected from  $T \leq 750$  °C onward (coinciding with the present  $T$  range), oxide degradation resulting from POA in O-free ambient is firmly correlated with SiO formation.<sup>16</sup> Defects (in the oxide network) may play a role in this. (6) The present results unveil interface degradation as a uniform substantial rupture of interfacial Si bonds, indicating that the degradation process initiates at the interface.

Degradation of dry Si/SiO<sub>2</sub>, driven by SiO formation, may then consistently be pictured as follows. During POA at  $T > 640$  °C in an O-free ambient [or partial O<sub>2</sub> pressure  $p_{\text{O}_2} < 100 p_{\text{SiO}}$  (Ref. 16)], Si terraces are attacked through SiO release. This SiO is either absorbed in the SiO<sub>2</sub> layer or escapes to the ambient through channels encountered in dry oxides.<sup>21</sup> The ensuing reduction in steps, leaving less room for interfacial adaptation, is accounted for by nature through additional interfacial Si bond rupture ( $P_b$  creation). In a way, it may be pictured as breakdown in interlayer connectivity. The specific amount of  $P_b$  created is set by the intricate balance between the change in interface free energy, interfacial oxide relaxation, and efficiency of SiO drainage. This results in a characteristic equilibrium number of  $N_C$  for each  $T$ .

The observations are also considered important for the general ESR spectroscopy of interface defects in Si/SiO<sub>2</sub> structures in that they may clarify the discrepancies over various ESR works in reported  $P_b$  densities for nominally identical Si/SiO<sub>2</sub> structures.<sup>2,4,10,22</sup> It is clear from the present data that, while the oxidation conditions may appear identical, postoxidation thermal processing in an inert or O-deficient ambient may altogether be far more dominant in setting the scene for  $P_b$  densities. Taken together with a varying degree of often inadvertent admixing of partial H passivation, an obvious explanation results. This serves as a warning in consistent (ESR) interface defect analysis that there is a third prominent factor to be held under strict control: beside the precise oxidation conditions (dry-wet,  $T_{\text{ox}}$ , etc.) and the H-passivation factor, there is the factor POA budget in an inert ambient.

In conclusion, the mechanism of an inert ambient POA-induced Si/SiO<sub>2</sub> interface degradation has been isolated as production of  $P_b$  interface defects, i.e., interfacial Si bond rupture. The crucial degrading step is found to be thermal

treatment in O-deficient ambient at temperatures in excess of  $\sim 660$  °C, where interfacial SiO(*g*) release is seen as the atomic driving force. A consistent overall model of POA-induced oxide-interfacial degradation has been attained. The importance of understanding this afflicting effect for device technology needs little comment. When referring to the det-

perimental properties of  $P_b$  defects as current degrading interface states, the message is clear. Thermal treatment of vital Si/SiO<sub>2</sub> interfaces in O-deficient ambient at elevated temperatures, even for short times, should be avoided at all times, unless followed by a curing post-thermal treatment reoxidation step.

- 
- <sup>1</sup>See, e.g., B. E. Deal, J. Electrochem. Soc. **121**, 198C (1974).  
<sup>2</sup>A. Stesmans, Phys. Rev. B **48**, 2418 (1993).  
<sup>3</sup>See, e.g., E. H. Poindexter and P. J. Caplan, Prog. Surf. Sci. **14**, 201 (1983).  
<sup>4</sup>P. J. Caplan, E. H. Poindexter, B. E. Deal, and R. R. Razouk, J. Appl. Phys. **50**, 5847 (1979).  
<sup>5</sup>K. L. Brower, Appl. Phys. Lett. **43**, 1111 (1983).  
<sup>6</sup>W. E. Carlos, Appl. Phys. Lett. **50**, 1450 (1987).  
<sup>7</sup>A. H. Edwards, Phys. Rev. B **36**, 9638 (1987); M. Cook and C. T. White, *ibid.* **38**, 9674 (1988).  
<sup>8</sup>See, e.g., P. Balk, Extended Abstracts Electronic Division Spring Meeting of the Electrochemical Society, San Francisco, 1965. Abstract No. 109 [J. Electrochem. Soc. **14**, 237 (1965)]; A. G. Revesz, K. H. Zaininger, and R. J. Evans, J. Phys. Chem. Solids **28**, 197 (1967).  
<sup>9</sup>K. L. Brower, Phys. Rev. B **38**, 9657 (1988).  
<sup>10</sup>K. L. Brower, Phys. Rev. B **42**, 3444 (1990).  
<sup>11</sup>K. L. Brower and S. M. Myers, Appl. Phys. Lett. **57**, 162 (1990).  
<sup>12</sup>A. H. Edwards, Phys. Rev. B **44**, 1832 (1991).  
<sup>13</sup>A. Stesmans, Appl. Phys. Lett. **68**, 2723 (1996).  
<sup>14</sup>See, e.g., D. M. Brown and P. V. Gray, J. Electrochem. Soc. **115**, 760 (1968); F. J. Montillo and P. Balk, *ibid.* **118**, 1463 (1971).  
<sup>15</sup>A. Stesmans and G. Van Gorp, Phys. Rev. B **42**, 3765 (1990).  
<sup>16</sup>K. Hofman, G. W. Rubloff, and D. R. Young, J. Appl. Phys. **61**, 4584 (1987).  
<sup>17</sup>DIMES, Delft, the Netherlands.  
<sup>18</sup>F. M. Ross and J. M. Gibson, Phys. Rev. Lett. **68**, 1782 (1992).  
<sup>19</sup>J. M. Gibson, M. Y. Lanzerotti, and V. Elser, Appl. Phys. Lett. **55**, 1394 (1989).  
<sup>20</sup>P. O. Hahn and M. Henzler, J. Appl. Phys. **52**, 4122 (1981).  
<sup>21</sup>E. A. Irene, J. Electrochem. Soc. **125**, 1708 (1978).  
<sup>22</sup>J. H. Stathis and L. Dori, Appl. Phys. Lett. **58**, 1641 (1991).